PERGAMON

International Journal of Multiphase Flow 27 (2001) 379–390

International Journal of Multiphase Flow

www.elsevier.com/locate/ijmulflow

Phase distributions for upward laminar dilute bubbly flows with non-uniform bubble sizes in a vertical pipe

Qiang Song*, Rui Luo, Xian Yong Yang, Zhou Wang

Department of Thermal Engineering, Tsinghua University, Beijing, 100084, People's Republic of China

Received 14 July 1999; received in revised form 14 March 2000

Abstract

Phase distributions were studied experimentally in fully developed laminar bubbly flow with non-uniform bubble sizes. A stereo-photographic method was designed to determine the three-dimensional position and size of each bubble in the flow field. The void fraction distributions were determined for every group bubble with approximately uniform size. The phase distributions for uniform bubble flows were also measured for analysis of the effect of the bubble size on the behaviour of the bubbly flows. The results show that if the average bubble diameter of a group of bubbles is less than about 3.5 mm, the void fraction distribution will peak near the pipe wall for both uniform and non-uniform bubble flows. For non-uniform bubble flows, large bubbles with diameters over about 3.7–3.8 mm create a void fraction profile with a peak near the pipe center. Bubbles with diameters from 3.5 to 3.8 mm tend to be distributed in a two-peak profile. The strong effect of bubble size on void fraction profiles is similar to that observed in previous investigations despite considerable differences in pipe size and working liquid properties.

Keywords: Laminar bubbly flow; Non-uniform bubble sizes; Phase distribution; 3D photography

1. Introduction

Laminar bubbly flow is a basic two-phase problem and a good example of the successful application of the two-fluid modeling, the most advanced theory for two-phase flow (Antal et al., 1991). However, although laminar bubbly flow may be the simplest flow pattern in gas–

* Corresponding author.
E-mail address: yyduan@te.tsinghua.edu.cn (Q. Song).

0301-9322/01/$ - see front matter
PII: S0301-9322(00)00025-2

liquid two-phase flow, its dynamic and kinetic behaviours are not yet understood completely. Previous experimental investigations show that the void fraction, one of the most important parameters to describe the inter-phase interactions in bubbly flow, has various distributions under different flow conditions (Valukina et al., 1979). Nakoryakov et al. (1996) observed that the void fraction distribution has a peak near the pipe wall if the bubble diameter is about 2 mm for bubbly flow in a 14.8 mm i.d. pipe. For the bubble diameters greater than about 3.6 mm, the void fraction distribution peak shifted to the pipe center. Kashinky et al. (1993) found a two-peak void fraction distribution in laminar bubbly flows with average void fractions of 0.01–0.02 and bubble diameters of around 2.3 mm. We can conclude that the bubble size has a tremendous effect on the phase distribution in bubbly flow.

For laminar bubbly flow with non-uniform bubble sizes, it is not difficult to predict that the phase distribution will be more complex. This implies more sophisticated mechanisms for the phase interactions and the interactions among bubbles, which requires further study to facilitate flow analysis. However, non-uniform bubble sizes present both experimental and theoretical difficulties because a variety of large and small bubbles means there is no longer a fixed relationship between the local void fraction and the local interfacial area concentration. The interfacial area concentration and void fraction will not have the same distributions. The interfacial area concentration is the most important parameter for quantifying the phase interactions, so the interfacial area concentration or the local average bubble diameter, together with the void fraction, is needed to describe the phase distribution. Neither the local average bubble diameter nor the local interfacial area concentration are easily measured, though some remarkable progress has been made in this regard (Kataoka et al., 1986; Clark and Turton, 1988; Liu et al., 1996).

Furthermore, development of two-phase flow theory for bubbly flow with non-uniform bubble sizes is a serious challenge. The two-fluid theory has not yet produced a model to predict the interfacial area distribution independent of the void fraction. Most models assume that all bubbles are divided into several groups and then the bubbles in each group are treated as of uniform size (Drew, 1983; Carrica et al., 1999). Therefore, this treatment seeks to measure the void fraction distribution for each bubble size group.

This paper describes measurements of the phase distributions of laminar bubbly flow using a specially designed three-dimensional (3D) photographic method. The position and size of each bubble in the flow field is determined. Then the void fraction distribution for each group bubbles with the same size is decided.

2. Experimental

2.1. Experimental loop

Experiments were performed in an oil–air test loop. The vertical test section was about 3.7 m long with an inner diameter, D, of 29 mm. Mineral oil was used as the liquid phase. The liquid flow rate was measured by a flow meter that was calibrated to a relative error of less than 2%. The airflow rate was measured by a rotameter with accuracy better than 5%. Air bubbles were generated by a small group of nozzles. A few combinations of different size

nozzles were used to produce bubbly flows with non-uniform bubble size distributions. The distance between the bubble generator and the measurement section was about $80D$ to ensure that the bubbly flows in the measurement section were fully developed.

A cooling system controlled the liquid phase temperature at $20 \pm 0.3^{\circ}C$ during the experiments. The liquid density, ρ_L, at $20^{\circ}C$ is 866 kg/m^3. The liquid dynamic viscosity, μ_L, is 3.16×10^{-2} Pa·s. The surface tension, σ_L, is 46.5×10^{-2} N/m.

2.2. Measurement method

A special 3D photographic method was designed to measure the phase distributions. The optical deformation caused by the liquid-filled circular pipe was eliminated by surrounding the measurement section of the pipe with a shroud box made of the pipe material and filling the gap between the box and the pipe with the working liquid. As shown in Fig. 1, a mirror reflects the side view from the y-direction on the x-direction. The photographs of the flow were taken by a camera from the x-direction, so the side and front views of the flow field were obtained simultaneously. Then the bubble position in the 3D flow field was determined by matching the side view image of the bubble to its front view image. The method for determining the bubble position has been described in detail by Luo et al. (1999).

A typical side-front view photograph of a bubble flow is shown in Fig. 2(a). The matching result for the flow is given in Fig. 2(b). In Fig. 2(b), a circle stands for a bubble that has been matched successfully. If a bubble in the side view has been matched to two or more bubbles in the front view, then these bubbles are marked by a cross. There is at least one mismatched bubble for two re-matched bubbles.

After the positions of all the bubbles in the flow field are determined, the void fraction distribution can be calculated as

$$\varepsilon(r) = \frac{\sum_{i=1}^{n} S_i(r)}{S_0(r)} \tag{1}$$

where $\varepsilon(r)$ is the radial void fraction profile, $S_0(r)$ is the surface area of an annulus which is

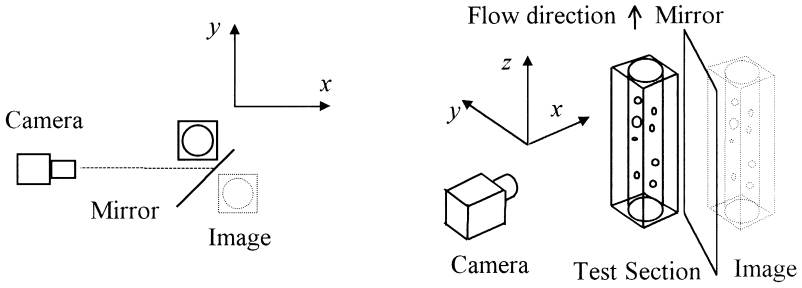

(a) Top view (b) Perspective view

Fig. 1. Arrangement of 3D photographic system: (a) top view; (b) perspective view.

coaxial with the pipe with radius r, n is the number of bubbles cut by the annulus, and $S_i(r)$ is the cross-sectional area of bubble i cut by the annulus. Since bubbles in the flow field will be deformed by the shear stress, they should be all ellipsoids. Then the bubble cross-sections cut by the annulus should be ellipses. The long- and short-axis lengths and their direction angles for all bubbles are measured from the photographs and are used to calculate $S_i(r)$ by

$$S_i(r) = \pi l_{ai}(r) l_{bi}(r) \tag{2}$$

$$l_{ai}(r) = \sqrt{l_{ai}^2 - \left(\sqrt{x_i^2 + y_i^2} - r\right)^2} \tag{3}$$

$$l_{bi}(r) = \sqrt{l_{bi}^2 - \frac{l_{bi}^2}{l_{ai}^2}\left(\sqrt{x_i^2 + y_i^2} - r\right)^2} \tag{4}$$

where l_{ai} and l_{bi} are the lengths of the long and short axes of bubble i, respectively.

2.3. Error analysis

The photographic technique is considered to be an absolute and standard method for two-phase flow measurements (Hewitt, 1978), which is usually used to calibrate other methods such

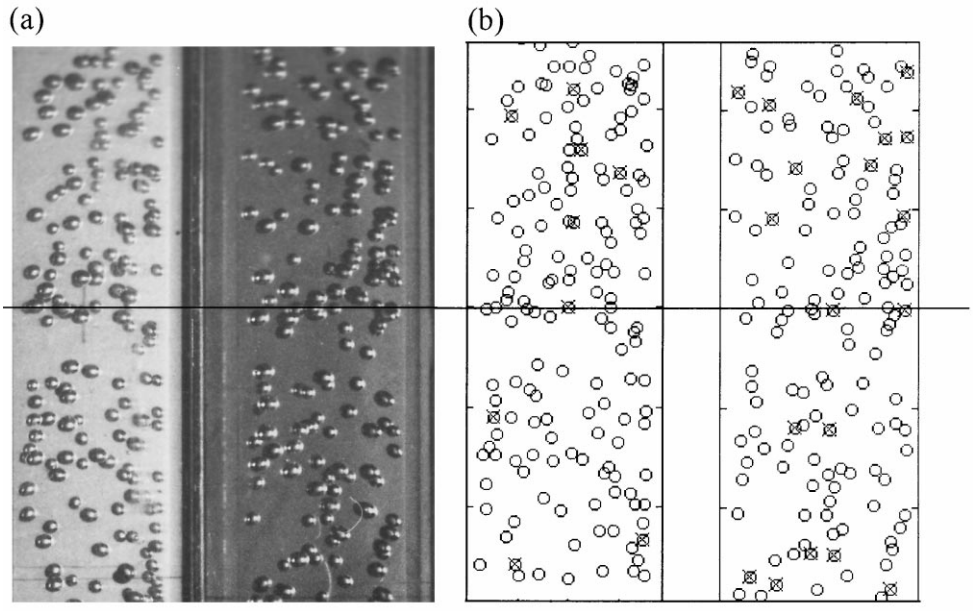

Fig. 2. A side-front view photo of the bubble flow (Test 12) and its matching result: ○, a bubble; ×, a bubble mismatched or re-matched: (a) side (left), front view photo; (b) matching result.

as probes, in particular for low void fraction flows (Revankar and Ishii, 1992). However, measurement errors occur in the 3D photographic method as discussed below.

The measurement errors consist of three parts. The first part is from mismatching between bubble images in the side and front views of the bubbly flow. The mismatching leads to incorrect determinations of the positions of those bubbles, which results in errors of the calculated phase distribution. Usually the mismatched bubbles account for less than 7–8% of total bubbles for most measured bubbly flows. To analyze the effect of the mismatching on the accuracy of the measured phase distribution, an artificial error was introduced into the matching process and caused 12% of the bubbles to be mismatched. The change in the void fraction distribution due to this artificial error was less than 5% (Luo et al., 1999). So, the 7–8% mismatches will lead to a phase distribution measurement error of about 3%.

The second source of error is due to the flow dynamics. Because of photographic analysis difficulties, a limited number of bubbles were used for each measurement. However, since the bubbly flows were steady laminar flows, there was no visible phase distribution fluctuation. For each measurement, three photographs were analyzed with 120–350 bubbles in each photograph. The difference in the bubble number between two photographs for the same flow is no greater than 6%, so the dynamic error of the phase distribution will be less than 5%. But for bubbly flows in which large bubbles tend to congregate in the center region of the pipe, the number of large bubbles may vary by more than 10% for different photographs of the same flow which will produce phase distribution errors for large bubbles of more than 10%.

The third part of the phase profile error is produced by imperfect estimates for the bubble deformation in the flows. The bubbles near the pipe wall are usually egg-shaped. The volume and area of an egg-shaped bubble was approximated by an ellipsoid with the same axial size, which gives volume and area errors of 3–4% for bubbles near the pipe wall.

In summary, the total phase distribution error is within 15% for most flows.

3. Experimental results and discussion

Fourteen tests were performed in total. The parameters and flow conditions for the eight

Table 1
Flow parameters for uniform bubble flow tests

Test no.	U_{SL} (m/s)	U_{SG} (m/s)	$U_{SG}/(U_{SL}+U_{SG})$	Average void fraction (%)	Average bubble diameter (mm)
1	0.27	0.0082	0.030	1.3	3.0
2	0.20	0.0082	0.040	1.7	3.3
3	0.13	0.0082	0.060	1.9	3.2
4	0.079	0.0082	0.090	2.0	3.3
5	0.27	0.0048	0.017	1.5	2.4
6	0.20	0.0048	0.023	2.1	2.7
7	0.13	0.0030	0.022	1.8	2.7
8	0.079	0.0030	0.034	1.6	2.8

tests with uniform bubble flows are summarized in Table 1 and for the six tests for non-uniform bubble flows in Table 2. The effect of bubble size on the phase distributions was deduced by artificially dividing the bubbles in each non-uniform bubble flow into large and small bubble groups according to a bubble size selected for each test.

3.1. General observations of bubbly flows

The two-phase pipe flow Reynolds numbers varied from 80 to 240 and the bubble rise Reynolds numbers varied from 2 to 40 in the present experiments. Therefore, the velocity fluctuation in the bubbly flows is small and the bubble motion relative to the liquid is linear if the void fraction is low and the interaction among bubbles is weak. Fig. 3(a) shows that the bubbles in Test 6 tended to line up and form clusters due to the Bernoulli effect of the bubble motion relative to the liquid. In this case, most bubbles aggregated in an annulus near the pipe wall due to the influence of the lateral force induced by the strong velocity gradient. This forms a high, sharp void fraction peak (see Fig. 4(c)). For the lower liquid velocities, Fig 3(b), the bubbly flows have a wider and lower void fraction distribution peak as discussed later, i.e. the bubbles can move with the liquid flow at different radial positions of the pipe. Since the bubbles near the pipe center have larger velocities than those near the pipe wall, the faster moving bubbles continuously pass the slow bubbles. As a result, the relative motions and

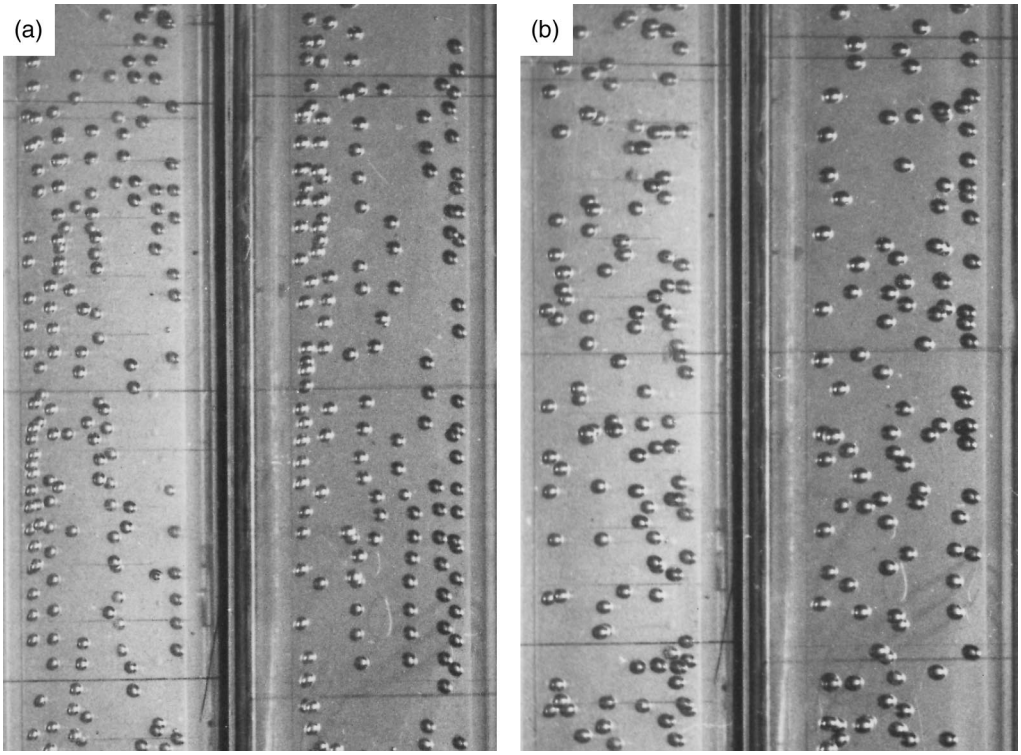

Fig. 3. Bubbly flows with clustered bubbles and non-clustered bubbles: (a) clustered bubbles in Test 6; (b) non-clustered bubbles in Test 3.

Table 2
Flow parameters for non-uniform bubble flow tests

Test no.	U_{SL} (m/s)	U_{SG} (m/s)	$U_{SG}/(U_{SL}+U_{SG})$	Average void fraction (%)		Average bubble diameter (mm)	
				Large bubble group	Small bubble group	Large bubble group	Small bubble group
9	0.19	0.013	0.062	1.0	1.9	3.9	3.0
10	0.26	0.013	0.046	0.8	2.0	3.9	3.1
11	0.079	0.0082	0.096	1.3	1.3	3.4	2.5
12	0.13	0.0082	0.060	1.6	1.0	3.2	2.4
13	0.19	0.0082	0.041	1.5	0.7	3.0	2.3
14	0.26	0.0082	0.030	1.4	0.7	3.1	2.2

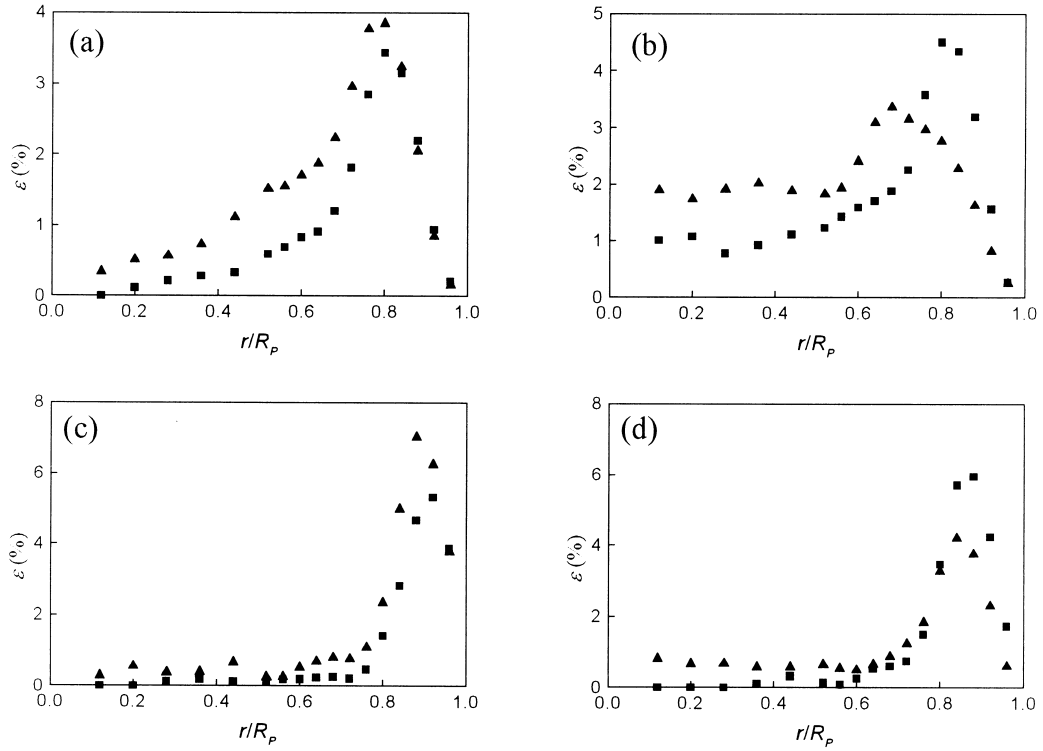

Fig. 4. Radial void fraction distributions for uniform bubble flows (R_P, pipe radius; ε- void fraction): (a) ■ for Test 1 and ▲ for Test 2; (b) ■ for Test 3 and ▲ for Test 4; (c) ■ for Test 5 and ▲ for Test 6; (d) ■ for Test 7 and ▲ for Test 8.

interactions among the bubbles will disturb the flow field and shatter the bubble clusters as shown in Fig. 3(b). For bubbly flows with non-uniform sizes, the bubble–bubble interactions are even stronger because the large and small bubbles may have totally different distributions, and so no long and stable bubble clusters, like ones shown in Fig. 3(a), were observed in non-uniform bubble flows, as shown in Fig. 2(a). However, some short bubble clusters consisting of three to five small bubbles can exist in the region near the pipe wall particularly for higher velocity non-uniform bubble flows.

In the present experiments, two nearly spherical bubbles cannot approach close enough to collide and coalesce regardless of whether they are in a cluster or not. This is because the liquid was not deliberately purified and might contain surfactants which make two approaching bubbles bounce away (Duineveld, 1998). Furthermore, unlike bubbles rising in water, a bubble moving in a viscous liquid has a thick boundary layer and a steady wake, which prevents two bubbles from approaching each other too close in a laminar flow field. However, as the bubble size increases, bubbles will have noticeable deformation and finally become cap-shaped. A cap-shape bubble rises slowly in a zig-zag path along the pipe-center axis. Small bubbles behind this large cap-shape bubble move faster and finally catch it, coalescing with the large bubble and further increasing its size. This is the beginning of the transition from bubbly flow to slug flow (Kalkach-Navarro et al., 1994).

3.2. Experimental results for uniform bubble flows

The void fraction profiles for uniform bubble flows are shown in Fig. 4(a)–(d). All void fraction profiles have peaks near the pipe wall. No center-peaked void fraction profiles were observed because the bubble sizes for all the uniform bubble flow tests were smaller than 3.4 mm. A center-peaked void fraction profile requires bubble diameters greater than 3.5 mm for bubbly flow even in a 14.8 mm i.d. pipe (Nakoryakov et al., 1996).

The results in Fig. 4 show that the void fraction profiles mainly depend on the bubble size and liquid velocity. The void fraction profile peaks move to the pipe wall as the bubble size decreases and the liquid velocity increases. In addition, the void fraction profile peak is higher and slimmer if the liquid phase velocity is large and the average void fraction is low. This may imply that the phase distribution is dominated by the lateral forces on the bubbles induced by the mean liquid velocity gradient and the wall–bubble interaction. On the other hand, for a low liquid velocity and high void fraction flow like Test 4, the void fraction profile has a wider and lower peak, which means that, even in low void fraction flows, the interactions among bubbles play an important part in the phase distribution shape. The interaction among bubbles modifies the pressure field due to the liquid flowing around a bubble. Then, higher pressures in regions with higher local void fraction will push bubbles to regions with lower void fractions (Antal et al., 1991).

3.3. Experimental results for non-uniform bubble flows

The measured phase and bubble size distributions in non-uniform bubble flows are shown in Fig. 5 (a)–(f). The results show that the void fraction profiles in non-uniform bubble flows are more complex than those in uniform bubble flows. As some large bubbles in Tests 9–11 have

diameters larger than about 3.5 mm, the void fraction profiles for these bubbles have a peak near the pipe center. The void fraction profile for the small bubbles still peaks near the pipe wall despite the large bubble void fraction profile. But the void fraction profile peak for the small bubbles becomes wider and lower in comparison with that for uniform bubble flows with

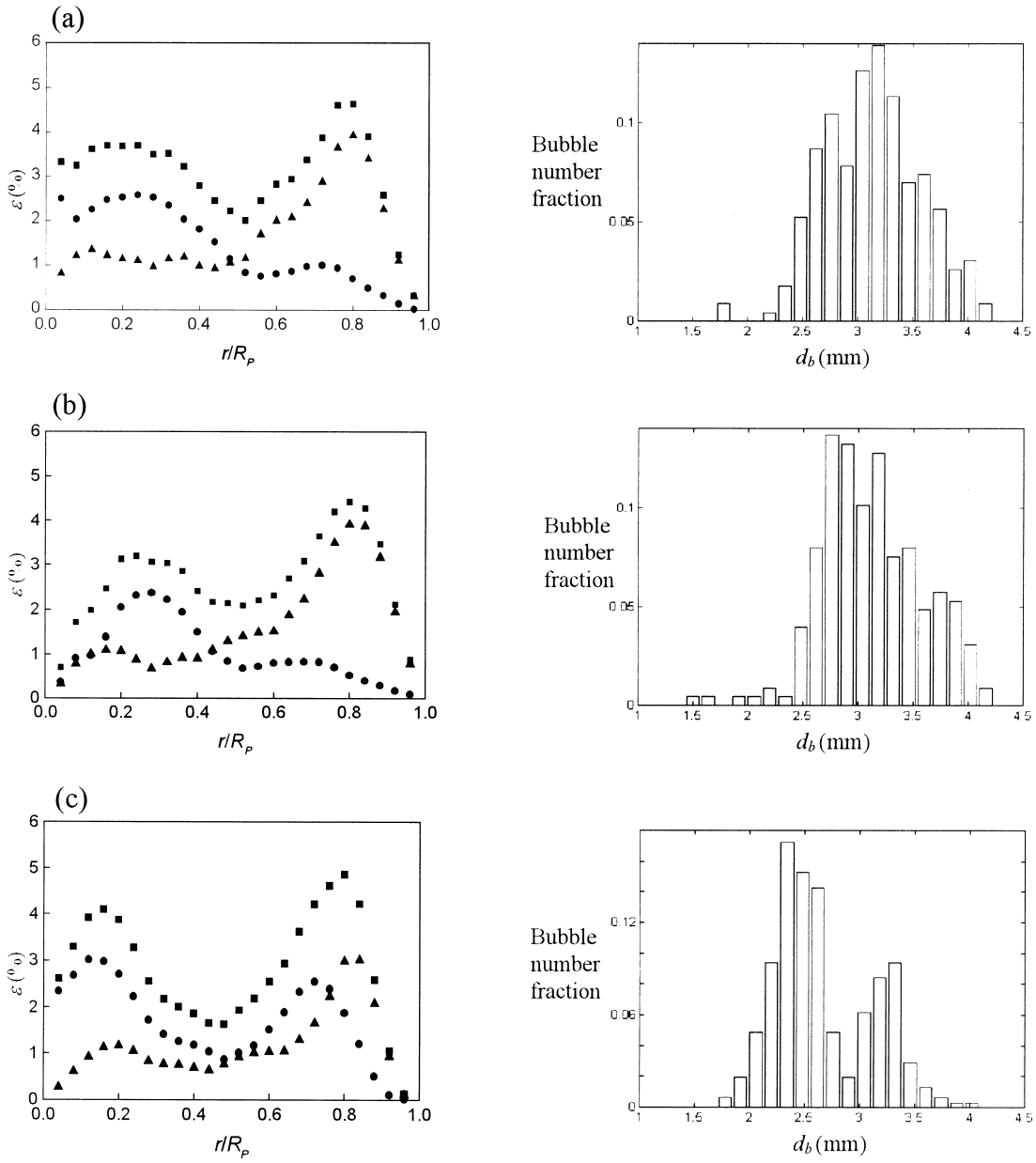

Fig. 5. Radial void fraction distributions (left) and corresponding bubble size distributions (right) for non-uniform bubble flows: ■, overall void fraction; ●, void fraction of large bubble group: ▲, void fraction of small bubble group: (a) Test 9; (b) Test 10; (c) Test 11; (d) Test 12; (e) Test 13; (f) Test 14.

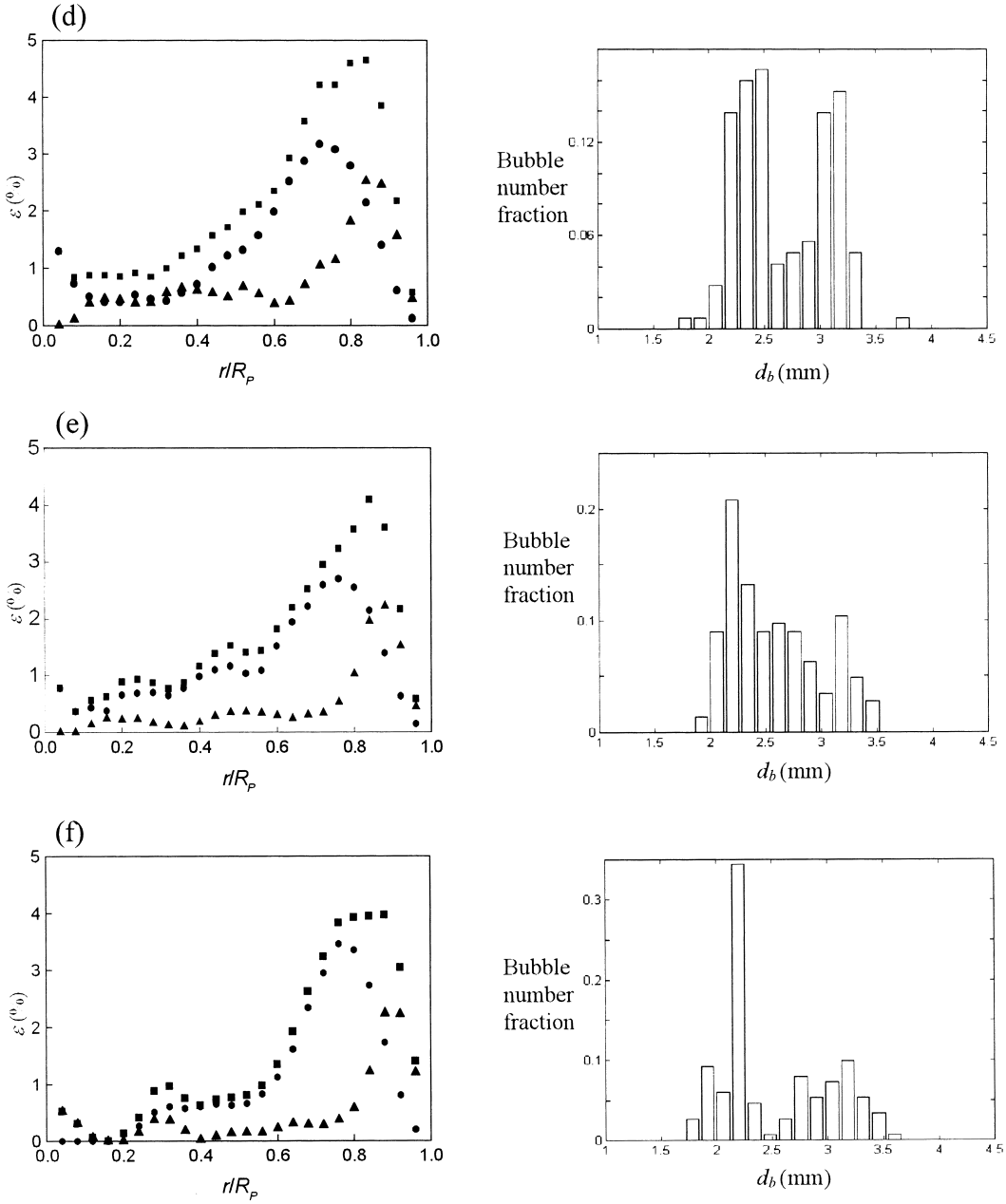

Fig. 5 (*continued*)

the same flow conditions. One reason for this may be that the interactions between the small and large bubbles make bubbles "diffuse" due to the modified pressure field discussed in the previous section. Another important reason may be that the group of large bubbles may disturb the liquid velocity distribution and create a more intense fluctuating flow field which

would cause all bubbles to diffuse in the flow field to reduce effect of the lateral force on bubbles.

The two-peak void fraction profile for the large bubbles was observed in a non-uniform bubble flow, Test 11, as shown in Fig. 5(c). It is similar to that observed by Kashinsky et al. (1993) in uniform bubble flows in a 14.8 mm i.d. pipe with void fractions of 0.01–0.02 and bubble diameters of 2.4–2.6 mm. No completely center-peaked void profiles as observed by Nakoryakov et al. (1996) were found in our experiments, perhaps because our pipe diameter was twice theirs. A totally center-peaked void fraction profile may require relatively large bubble diameters in a large pipe.

4. Conclusion

The bubble size has a dominant effect on the phase distribution. The void fraction profiles for bubbles with diameters less than 3.5 mm are wall-peaked for all uniform and non-uniform bubble flows in the present experiments. For bubble diameters larger than 3.7–3.8 mm, the bubble void fraction profiles have peaks near the pipe center. Bubbles between 3.5 and 3.7 mm have a two-peak profile. The results are similar to those of Nakoryakov et al. (1996) and Kashinsky et al. (1993) under considerably different experimental conditions.

The bubbly flows with non-uniform bubble sizes have more complex and varied phase distributions. The bubbles with different sizes have different phase distributions in the same bubbly flow. The different phase distributions for the small and large bubbles create a more intense fluctuating flow field that suppresses the effect of the lateral force on the bubbles and then flattens void fraction profile peaks near the pipe wall. At the same time, the interactions among bubbles also cause the bubbles to diffuse producing a void fraction profile with a wider and lower peak even in low void fraction flows.

Acknowledgements

This research was supported by the National Natural Science Foundation of China (Grant No. 19572042).

References

Antal, S.P., Lahey Jr, R.J., Flaherty, J.E., 1991. Analysis of phase distribution in fully developed laminar bubbly two-phase flow. Int. J. Multiphase Flow 17, 635–652.

Carrica, P.M., Drew, D., Bonetto, F., Lahey Jr., R.T., 1999. A polydisperse model for bubbly two-phase flow around a surface ship. Int. J. Multiphase Flow 25, 257–305.

Clark, N.N., Turton, R., 1988. Chord length distribution related to bubble size distribution in multiphase flows. Int. J. Multiphase Flow 14, 413–424.

Drew, D.A., 1983. Mathematical modeling of two-phase flow. Annual Review of Fluids Mechanics 42, 545–570.

Duineveld, P.C., 1998. Bouncing and coalescence of bubble pairs rising at high Reynolds number in pure water or aqueous surfactant solutions. Applied Scientific Research 58, 409–439.

Hewitt, G.F., 1978. Measurement of Two Phase Flow Parameters. Academic Press, New York.
Kalkach-Navarro, S., Lahey Jr, R.T., Drew, D.A., 1994. Analysis of the bubbly/slug flow regime transition. Nuclear Eng. and Des. 151, 15–39.
Kashinsky, O.N., Timkin, L.S., Cartellier, A., 1993. Experimental study of 'laminar' bubbly flows in a vertical pipe. Experiments in Fluids 14, 308–314.
Kataoka, I., Ishii, M., Serizawa, A., 1986. Local formulation and measurements of interfacial area concentration in two-phase flow. Int. J. Multiphase Flow 12, 509–529.
Liu, W., Clark, N.N., Karamavrue, A.I., 1996. General method for the transformation of chord-length data to a local bubble-size distribution. AICHE Journal 42, 2173–2720.
Luo, R., Song, Q., Yang, X.Y., Wang, Z., 1999. A three-dimensional photographic method for measurement of phase distribution in bubbly flow. Measurement Science and Technology, in press.
Nakoryakov, V.E., Kashinsky, O.N., Randin, V.V., Timkin, L.S., 1996. Gas–liquid bubbly flow in vertical pipes. Journal of Fluid Engineering 118, 377–382.
Revankar, S.T., Ishii, M., 1992. Local interfacial area measurement in bubbly flow. Int. J. Heat and Mass Transfer 35, 913–925.
Valukina, N.V., Kozmenko, B.K., Kashinsky, O.N., 1979. Characteristics of a flow of monodisperse gas–liquid mixture in a vertical pipe. Journal of Engineering Physics 36, 695–699.